



The effect of salts on molecular mobility in amorphous sucrose monitored by erythrosin B phosphorescence

Yumin You, Richard D. Ludescher *

Department of Food Science, Rutgers, The State University of New Jersey, 65 Dudley Road, New Brunswick, NJ 08901-8520, United States

ARTICLE INFO

Article history:

Received 3 March 2008

Received in revised form 3 June 2008

Accepted 6 June 2008

Available online 14 June 2008

Keywords:

Molecular mobility

Dynamic site heterogeneity

Sucrose glass

Undercooled liquid

ABSTRACT

Salts are present in most amorphous biomaterials such as dried or frozen solid foods, plant seeds, and bacterial spores, and in some pharmaceutical formulations. However, knowledge of how salts modulate the physical properties of amorphous solid sugars, a major component in these systems, is lacking. We have used phosphorescence of the triplet probe erythrosin B (Ery B) to monitor molecular mobility in amorphous sucrose films (dried against P_2O_5) containing the salts NaCl, $MgCl_2$, $CaCl_2$, NaAcetate, $Na_3Citrate$, NaH_2PO_4 , or Na_2HPO_4 at a mole ratio of 0.2:1 (salt/sucrose). All the salts examined, except NaH_2PO_4 , significantly increased the phosphorescence lifetime of Ery B over the temperature range from 5 to 100 °C. This increase is due to a reduction in the rate of collisional quenching of the triplet state due to interactions with the matrix, indicating that these salts decreased the matrix molecular mobility. NaAcetate, $Na_3Citrate$, and Na_2HPO_4 decreased mobility more than NaCl, $CaCl_2$, or $MgCl_2$, perhaps due to specific hydrogen bonding interactions between the anion and sucrose. Systematic variations in the probe emission lifetime across the excitation and emission bands at 25 °C indicate that there are sites of different mobilities within amorphous solid sucrose; this dynamic site heterogeneity was enhanced in the presence of the divalent cationic salts $MgCl_2$ and $CaCl_2$. These results suggest that salts may play a significant role in modulating the mobility, and thus the long-term stability, of amorphous biological matrices.

© 2008 Elsevier Ltd. All rights reserved.

1. Introduction

Molecular mobility plays an important role in modulating the physical properties of amorphous solids and thus in modulating the stability and the shelf life of foods, pharmaceuticals, and biomaterials.^{1–3} Amorphous solids soften at the glass transition temperature (T_g) due to activation of large-scale molecular motions (α relaxations) that underlie the onset of translational and large-scale rotational motions within the matrix. There are also secondary β relaxations within the glass which are activated at T_β and are related to vibrational and local side-chain rotational motions. The temperature-dependent molecular mobility controls the physical and chemical properties of amorphous biomaterials by modulating the nature and kinetics of reactions that occur during processing and storage.

The measurement of molecular mobility in amorphous sugars is of fundamental interest because it provides a straightforward way to evaluate stability or potential shelf life. A number of techniques have been used to characterize the properties and mobility of amorphous materials.^{4–12} We have recently demonstrated that

phosphorescence of erythrosin B (Ery B) provides a sensitive indicator of molecular mobility as well as dynamic site heterogeneity in amorphous sugars^{13–16} and proteins.^{17–21}

Amorphous sucrose is involved in the protection of living organisms, seeds, and spores against stresses induced by desiccation;^{22–24} it is also the major component responsible for the stability of many dried and frozen foods. Its ability to protect biomaterials from freeze-thaw damage and to provide long-term storage stability has attracted considerable attention in an effort to understand the mechanisms of this stabilization and to develop stable solid state formulations for long-term storage of the labile compounds in foods and pharmaceuticals.

Since anhydrous glasses often consist of a variety of compounds, such as buffers and tonicity adjusters in pharmaceuticals and assorted small molecules in foods, interactions among component molecules may modulate the molecular mobility and other physical properties of amorphous sucrose.

A few studies have explored how salts modulate the stability of sugar glasses by studying their effect on the glass transition temperature T_g and molecule mobility. Izutsu and Aoyagi studied the effect of different inorganic salts on crystallization of poly ethylene glycol in frozen solutions.²⁵ They found that salts prevent crystallization by altering molecular interactions and reducing molecular mobility; the effect depends on the type of salt and concentration.

Abbreviations: Ery B, erythrosin B; T_g , glass transition temperature.

* Corresponding author. Tel.: +1 732 932 9611x231; fax: +1 732 932 6776.

E-mail address: ludescher@aesop.rutgers.edu (R. D. Ludescher).

Shalaev et al. studied the properties of pharmaceutically compatible buffers at sub-zero temperatures in lyophilized formulations and found that the T'_g of a freeze-dried system (the T_g of the maximally freeze-concentrated solid) results from a competition between two opposing actions: increased viscosity due to an increase in the electrostatic interaction and decreased viscosity due to an increase in the amount of unfrozen water.²⁶ Mazzobre et al. found that a combination of trehalose and divalent cations stabilized proteins in freeze-dried systems better than sugar alone.²⁷ Recently, You and Ludescher used phosphorescence of erythrosin B to investigate the effect of sodium chloride on the molecular mobility in amorphous sucrose matrix.²⁸ This salt reduces the matrix molecular mobility in a concentration-dependent manner, and this effect appeared to be opposed by a plasticization induced by increased residual water in the presence of higher amounts of salt.

In the present study, the effect of temperature on the phosphorescence lifetime of Ery B was used to monitor matrix mobility in amorphous sucrose films containing a variety of salts at a mole ratio of 0.2 salt/sucrose, a concentration chosen on the basis of our earlier results with NaCl. The results indicate that salts in general lower the matrix molecular mobility, suggesting that proper manipulation of salt composition may be an effective method of increasing stability and shelf life of amorphous foods, encapsulated ingredients, and pharmaceuticals.

2. Results

A series of chloride salts (NaCl, CaCl₂, and MgCl₂) and sodium salts (Na₃Citrate, NaAcetate, NaH₂PO₄, and Na₂HPO₄) were dispersed in an amorphous sucrose matrix at a salt/sucrose mole ratio of 0.2 and the matrix molecular mobility was monitored using phosphorescence from the triplet probe Ery B dispersed in the matrix at a probe/sucrose mole ratio of 10⁴. At this concentration each Ery B probe is surrounded by a sucrose layer on average 10–11 molecules thick. Previous work has established that Ery B does not aggregate under these conditions and reports the mobility of the unperturbed sucrose matrix.^{13,29} The data on the sucrose–NaCl matrix reported here have been published as part of a more extensive study of the effect of NaCl on sucrose matrix mobility;²⁸ they are included here for the sake of comparison.

2.1. Phosphorescence decay kinetics

Phosphorescence intensity decays of Ery B in sucrose and sucrose–salt glasses were measured over the temperature range from 5 to 100 °C during both heating and cooling cycles. Films were checked at each temperature under crossed polarizers to make sure that no crystallization occurred during the cooling cycle. Intensity decays at each temperature were well fit to a stretched exponential function (Eq. 1, Section 5) as expected for Ery B in sucrose;^{13,29} the stretched exponential lifetimes are plotted as a function of temperature during heating and cooling for pure sucrose and for sucrose with NaCl and CaCl₂ in Figure 1.

The lifetimes during heating and cooling were identical within error for pure sucrose and for sucrose–NaCl (Fig. 1a) but not for the other sucrose–salt films. Films containing CaCl₂, MgCl₂, Na₃Citrate, NaAcetate, and Na₂HPO₄ displayed pronounced hysteresis over the temperature interval from 95 °C to 35 °C; hysteresis in NaH₂PO₄ was less evident (only data for sucrose–CaCl₂ are shown in Fig. 1b). The lifetime during cooling in each film was equal to or greater than the lifetime during heating at each temperature. The shape of the hysteresis loop and the temperature interval over which the lifetimes differed depended on the type of salt. Lifetimes measured during a second heating cycle were identical with those

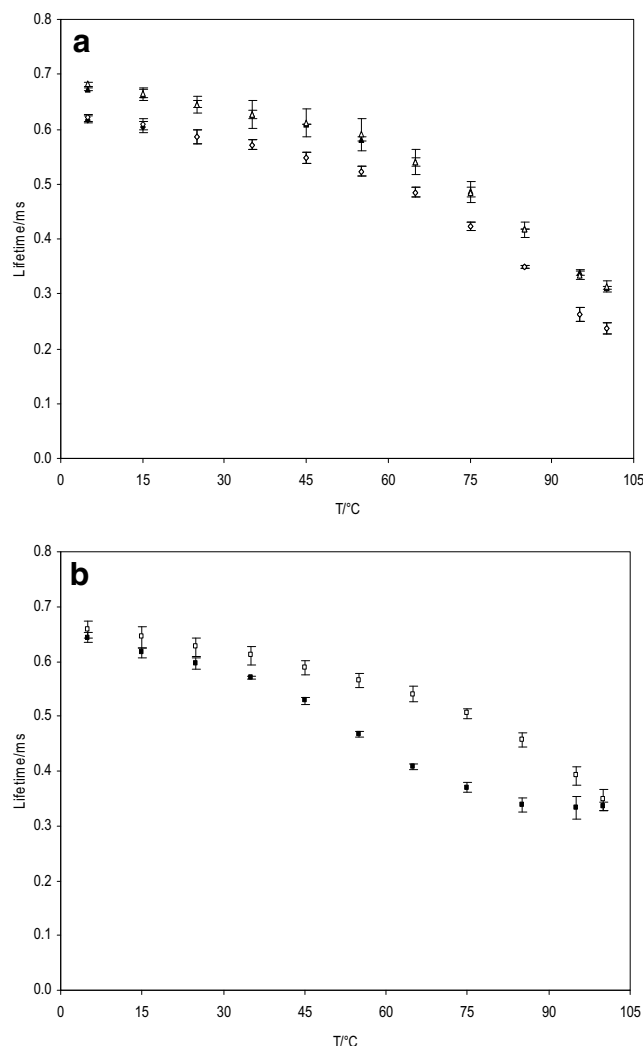


Figure 1. Phosphorescence lifetimes of erythrosin B in sucrose and sucrose–salt films as a function of temperature during heating (solid symbols) and cooling (open symbols) cycles. (a) Lifetimes in sucrose (◆, ◇) and in sucrose–NaCl film at 0.2 NaCl/sucrose mole ratio (▲, △). (b) Lifetimes in sucrose–CaCl₂ film at 0.2 CaCl₂/sucrose mole ratio (■, □).

measured during the first cooling cycle for films containing Na₃Citrate, indicating that hysteresis was not repeatable. The effect of salts on the matrix mobility thus appeared to be complicated by the presence of additional moisture retained during drying some salt-containing films. The residual moisture tended to increase the mobility, indicated by the lower lifetime values obtained during heating compared with higher lifetime values obtained during cooling. In order to monitor the effect of salt without interference from additional moisture, the lifetimes collected during cooling were thus used for subsequent mobility analysis.

The stretched exponential lifetimes and stretching exponents (β) from cooling data are plotted as a function of temperature for sucrose films containing NaCl, CaCl₂, and MgCl₂ (the chloride salts) in Figure 2a and b, respectively, and for sucrose films containing Na₃Citrate, NaAcetate, NaH₂PO₄, Na₂HPO₄, and NaCl (the sodium salts) in Figure 3a and b, respectively. Lifetimes were significantly higher in the presence of salt than in pure sucrose for all salts at all temperatures except for MgCl₂ at low temperature and NaH₂PO₄ over the entire temperature range. In general, the lifetime curve for the salt-containing matrix was approximately parallel to that for pure sucrose and displaced to higher lifetime. The temperature dependence of the lifetime displayed biphasic behavior in all

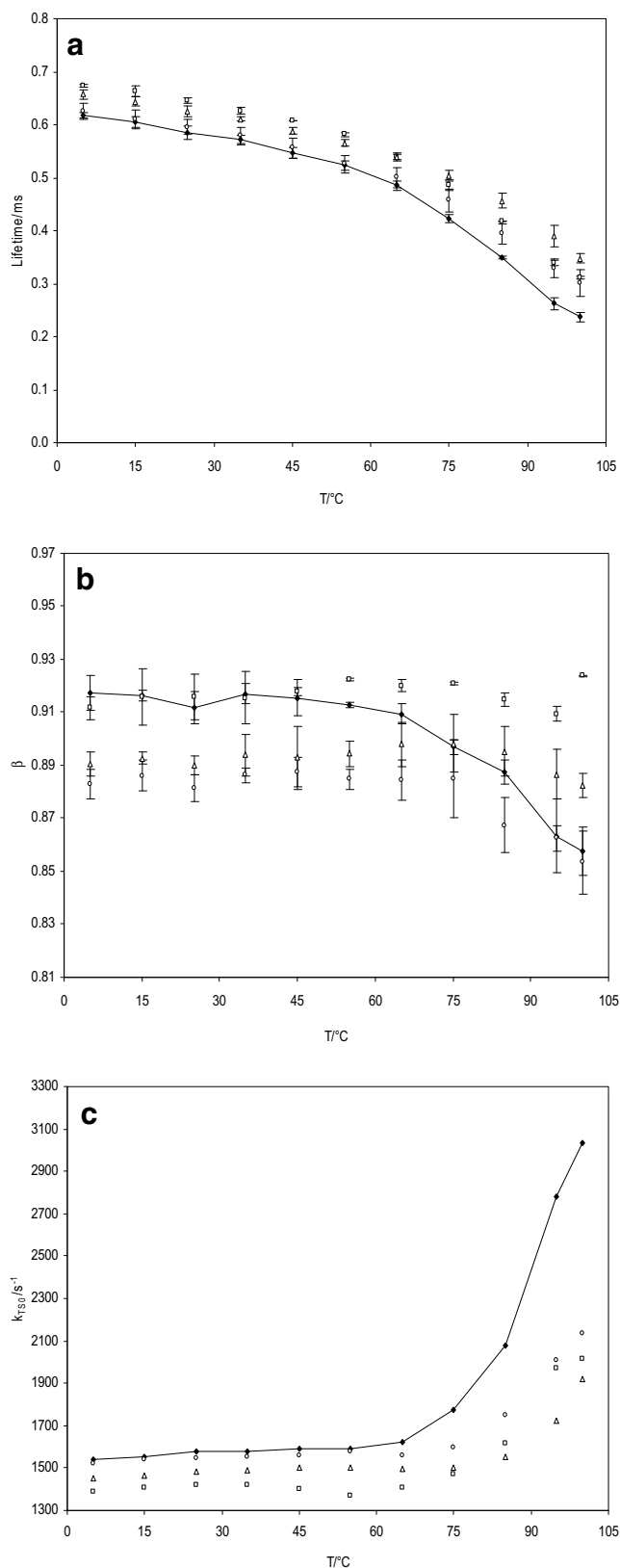


Figure 2. Temperature dependence of the lifetime (a) and stretching exponent β (b) obtained from fits to a stretched exponential function of the phosphorescence intensity decay of erythrosin B in amorphous sucrose-salt films with a salt/sucrose mole ratio of 0.2. Temperature dependence of the non-radiative decay rate k_{TS0} for the triplet state (c) in amorphous sucrose-salt films; see text for additional details. Phosphorescence intensity decay data collected from 100 to 5 °C (during cooling cycle). Data from pure sucrose (◆), sucrose-NaCl (□), sucrose-CaCl₂ (△), and sucrose-MgCl₂ (○).

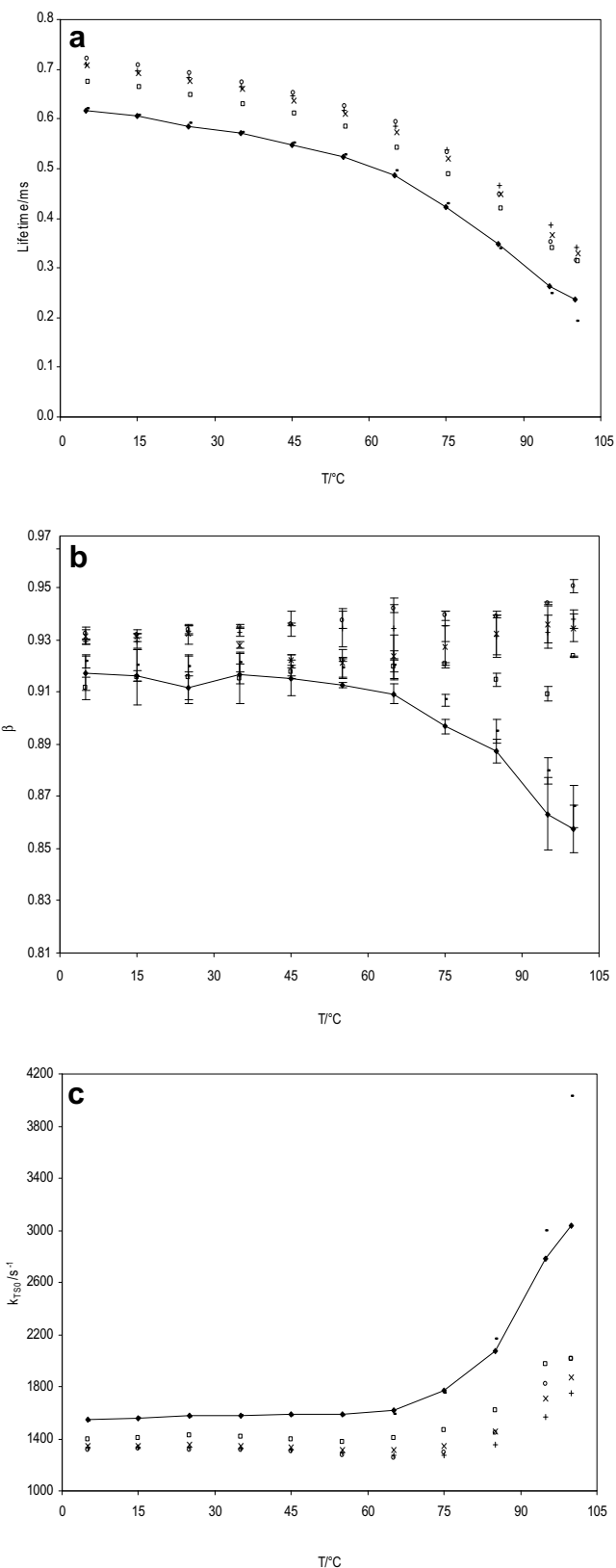


Figure 3. Temperature dependence of the lifetime (a) and stretching exponent β (b) obtained from fits to a stretched exponential function of the phosphorescence intensity decay of erythrosin B in amorphous sucrose-salt films with a salt/sucrose mole ratio of 0.2. Temperature dependence of the non-radiative decay rate k_{TS0} for the triplet state (c) in amorphous sucrose-salt films; see text for additional details. Phosphorescence intensity decay data collected from 100 to 5 °C (during cooling cycle). Data from pure sucrose (◆), sucrose-Na₃Citrate (+), sucrose-NaAcetate (○), sucrose-NaH₂PO₄ (-), sucrose-Na₂HPO₄ (×), and sucrose-NaCl (□).

matrixes, exhibiting a gradual linear decrease at low and a more steeply linear decrease at high temperature; the curves exhibited break points around the T_g of pure sucrose.

In the chloride salts, the lifetimes decreased in the order $\text{NaCl} > \text{CaCl}_2 > \text{MgCl}_2 \approx \text{sucrose}$ at low temperature and $\text{CaCl}_2 > \text{NaCl} > \text{MgCl}_2 > \text{sucrose}$ at high temperature. In the sodium salts, the lifetimes decreased in the order $\text{NaAcetate} \approx \text{Na}_3\text{Citrate} \geq \text{Na}_2\text{HPO}_4 > \text{NaCl} > \text{NaH}_2\text{PO}_4 \approx \text{sucrose}$ at low temperature and $\text{Na}_3\text{Citrate} \geq \text{NaAcetate} \approx \text{Na}_2\text{HPO}_4 > \text{NaCl} > \text{NaH}_2\text{PO}_4 \approx \text{sucrose}$ at high temperature.

The values of the stretching exponent β in all sucrose–salt films did not change significantly with temperature during the cooling cycle. The values of β decreased in the order $\text{NaAcetate} > \text{Na}_3\text{Citrate} \approx \text{Na}_2\text{HPO}_4 > \text{NaCl} > \text{NaH}_2\text{PO}_4 > \text{sucrose} > \text{CaCl}_2 > \text{MgCl}_2$.

The triplet state non-radiative quenching rate, k_{TSO} , was calculated from the phosphorescence lifetimes as described in Section 5; these values are plotted for the chloride salts in Figure 2c and for the sodium salts in Figure 3c. The rate k_{TSO} increased gradually at low temperature and more steeply at high temperature in all sucrose–salt mixtures. In the chloride salts, MgCl_2 had no significant effect on k_{TSO} below 65 °C but did have at higher temperatures, while CaCl_2 and NaCl decreased k_{TSO} both in the sucrose glass at $T < 65$ °C and in the undercooled liquid at higher temperatures. The magnitude of k_{TSO} varied in the rank order sucrose $\approx \text{MgCl}_2 > \text{CaCl}_2 > \text{NaCl}$ below 65 °C and sucrose $> \text{MgCl}_2 > \text{NaCl} > \text{CaCl}_2$ above 75 °C. In the sodium salts, all except NaH_2PO_4 had a significant and similar effect on the collisional quenching rate across the entire temperature range.

2.2. Spectral heterogeneity

Phosphorescence intensity decays of Ery B in sucrose films with different salts were measured as a function of excitation and emission wavelength at 25 °C during the heating cycle. All decays were well fit using a stretched exponential decay model; the lifetimes are plotted versus excitation and emission wavelength for the chloride salts in Figure 4a and for the sodium salts in Figure 5a. In all matrixes, lifetimes decreased with increasing wavelength across the emission band. In pure sucrose, the lifetimes varied from a high of 0.65 ms at 640 nm to a low of 0.52 ms at 720 nm; lifetimes also decreased monotonically with increasing wavelength in all the sucrose–salt films.

The effect of salts on the sucrose site heterogeneity was evaluated by comparing the fractional change of lifetime across the emission band $((\tau_{640} - \tau_{720})/\tau_{720})$. Compared with pure sucrose (0.24), the fractional change increased with CaCl_2 (0.30), MgCl_2 (0.30), and NaCl (0.29), decreased with $\text{Na}_3\text{Citrate}$ (0.21), NaAcetate (0.21), and Na_2HPO_4 (0.18), and remained unchanged with NaH_2PO_4 (0.25). The chloride salts thus appeared to increase site heterogeneity while the sodium salts, except for NaH_2PO_4 , tended to decrease the heterogeneity of sucrose matrix; the decrease in heterogeneity may also reflect the influence of hydrogen bonding anions.

Lifetimes also varied across the excitation band, increasing with increasing wavelength to a maximum at 520–540 nm and then decreasing at higher wavelengths. The variation of lifetime across the excitation band was similar in the presence of all salts.

The stretching exponent β (see Section 5.2) varied as a function of excitation and emission wavelength in both the chloride (Fig. 4b) and the sodium (Fig. 5b) salts. In both sucrose and the sucrose–salt films, β was lower at the blue edge of the emission band, increased with increasing wavelength to a maximum at 680–690 nm, and then decreased slightly at the red edge. In general for both excitation and emission, β was slightly lower than sucrose in the chloride salts but higher than sucrose in the sodium salts.

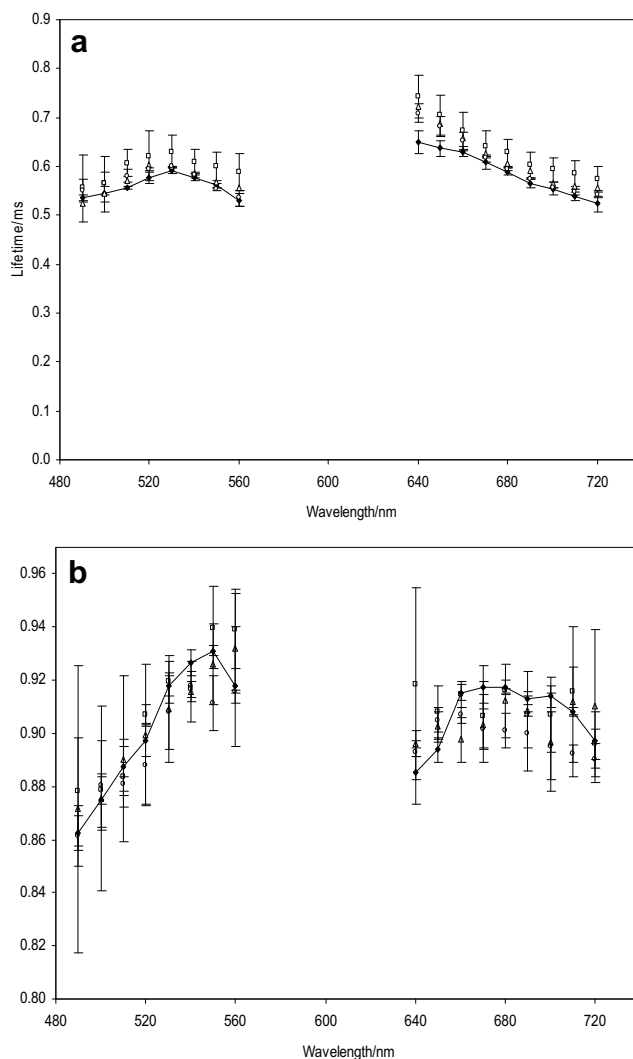


Figure 4. Lifetimes (a) and stretching exponents β (b) from fits to a stretched exponential function of intensity decays of erythrosin B in amorphous sucrose–salt films with a salt/sucrose mole ratio of 0.2:1 collected as a function of excitation wavelength (with 680 nm emission) and emission wavelength (with 530 nm excitation) at 25 °C. Data collected during heating from Ery B in sucrose films with various salts: \blacklozenge , sucrose; \square , sucrose– NaCl ; \triangle , sucrose– CaCl_2 ; \circ , sucrose– MgCl_2 .

The addition of salt appeared to slightly decrease the variation of β across both the excitation and the emission band.

The calculated matrix quenching rate k_{TSO} (see Section 5.3) is plotted versus excitation and emission wavelength for all sucrose–salt films in Figure 6. The collisional quenching rate increased with increasing emission wavelength in all films and the quenching rate was reduced below that in pure sucrose in the presence of nearly all salts. Although the effect of salt on the quenching rate varied somewhat with emission wavelength, in general the magnitude followed the rank order sucrose $\approx \text{NaH}_2\text{PO}_4 > \text{MgCl}_2 > \text{CaCl}_2 > \text{NaCl} > \text{Na}_2\text{HPO}_4 > \text{Na}_3\text{Citrate} > \text{NaAcetate}$. The quenching rate also varied across the excitation band, showing a minimum value around 530 nm and higher values at both the blue and red edge in films. The magnitude of k_{TSO} followed essentially the same rank order across the excitation band as that seen across the emission band.

3. Discussion

These spectroscopic data indicate that the phosphorescence of erythrosin B is sensitive to changes induced by salt in the physical

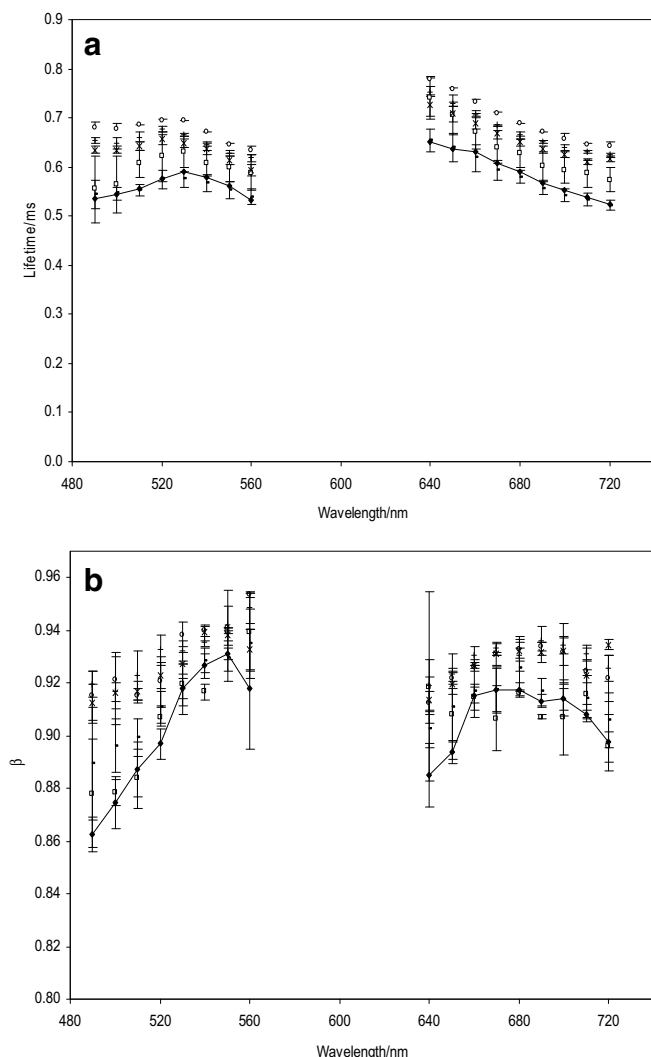


Figure 5. Lifetimes (a) and stretching exponents β (b) from fits to a stretched exponential model of intensity decays of erythrosin B in amorphous sucrose-salt films with a salt/sucrose mole ratio of 0.2:1 collected as a function of excitation wavelength (with 680 nm emission) and emission wavelength (with 530 nm excitation) at 25 °C. Data collected during heating from Ery B in sucrose films with various salts: \blacklozenge , sucrose; $+$, sucrose- $\text{Na}_3\text{Citrate}$; \circ , sucrose- NaAcetate ; $-$, sucrose- NaH_2PO_4 ; \times , sucrose- Na_2HPO_4 ; \square , sucrose- NaCl .

properties of amorphous solid sucrose matrix. Analysis of the temperature and wavelength-dependence of the lifetime of the probe dispersed in amorphous sucrose mixed with different salts provides insight into the solid state biophysics of the amorphous sucrose and the influence of salt on these biophysical properties.

3.1. Lifetime hysteresis

Lifetime curves as a function of temperature during heating and cooling exhibited hysteresis in all films except pure sucrose and sucrose- NaCl (Fig. 1). This hysteresis reflected fairly dramatic decreases in lifetime over the temperature range from ~ 35 to 85 °C during the heating cycle that were not present during the cooling cycle, decreases that reflected the activation of significant matrix mobility at lower temperatures. The residual water contents of the sucrose (0.56 wt %) and sucrose- NaCl (1.04 wt %) films, which did not exhibit hysteresis, were significantly lower than that of the other sucrose-salt films (2.8–4.3 wt %), which did exhibit hysteresis (see Section 5); in addition, hysteresis did not reoccur during a subsequent heating cycle in the sucrose- $\text{Na}_3\text{Citrate}$ film. A

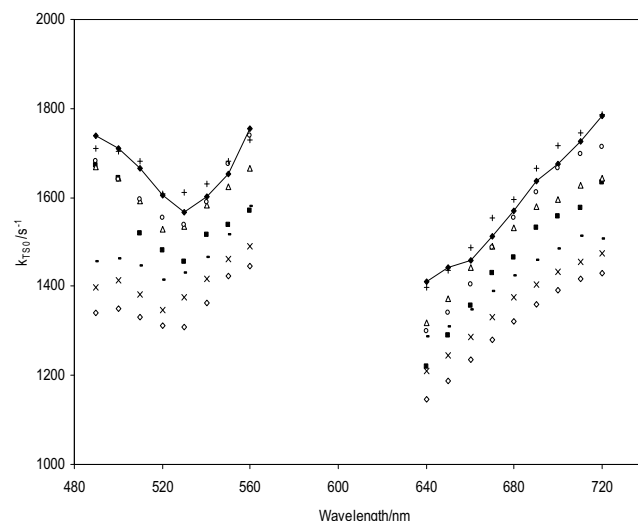


Figure 6. Rate constant for collisional quenching of the triplet state (k_{TSO}) as a function of excitation wavelength (with 680 nm emission) and emission wavelength (with 530 nm excitation) at 25 °C; calculated from data given in Figure 5. Data collected from Ery B in sucrose films with various salts: \blacklozenge , sucrose; \blacksquare , sucrose- NaCl ; \triangle , sucrose- CaCl_2 ; \circ , sucrose- MgCl_2 ; \times , sucrose- $\text{Na}_3\text{Citrate}$; \diamond , sucrose- NaAcetate ; $+$, sucrose- NaH_2PO_4 ; $-$, sucrose- Na_2HPO_4 .

heating/cooling cycle with equilibration at each target temperature was in fact an annealing treatment that facilitated migration of the residual water to the film surface to be removed by the flow of dry nitrogen. The lifetime measured during cooling was higher, indicating lower matrix mobility due to the loss of water. Transition temperatures, determined from Arrhenius plots of $\ln(1/\tau)$ versus $1/T$ using the lifetime collected during heating (calculated from the intersection of extrapolated linear behavior at low and high temperatures), decreased linearly with increasing water content in these samples (correlation coefficient of 0.959 or higher), confirming that the hysteresis reflected, at least in part, plasticization of the sucrose matrix by water. We thus conclude that the lower lifetimes seen during heating in sucrose- CaCl_2 (Fig. 1b) and other films reflected the extra mobility due to water plasticization of the sucrose matrix and that the hysteresis reflected loss of this water during heating. Consequently, the lifetimes collected during the cooling cycle represented the dynamics of a nearly dry (≤ 1 wt %) matrix and thus reflected the dynamic effect of salt on the sucrose matrix.

3.2. Salts make the sucrose matrix more rigid

The phosphorescence lifetime of Ery B provides information about the triplet state non-radiative quenching rates^{13,30,31} (see Section 5.3). The Ery B phosphorescence emission rate $k_{\text{P}} (=1/\tau)$ in the absence of oxygen is the sum of rates of radiative emission (k_{RP}), reverse intersystem crossing to the excited singlet S_1 state (k_{TS1}), and intersystem crossing to the ground singlet S_0 state (k_{TS0}). Since k_{RP} is 41 s^{-1} and constant,^{30,31} the increase of k_{P} (the decrease in lifetime) with temperature reflects an increase in both k_{TS1} and k_{TS0} . The variation in probe lifetime with addition of salt thus reflects variations in the total rate of non-radiative quenching ($k_{\text{TS1}} + k_{\text{TS0}}$). Since the value of k_{TS1} can be estimated (see Section 5.3), the effect of salt on the probe lifetime provides information on the effect of salt on k_{TS0} .^{13,15}

The magnitude of k_{TS0} reflects internal processes that determine the extent of vibrational coupling between the excited T_1 state and the ground S_0 state as well as external processes due to interactions between the probe molecule and its environment that affect how probe vibrational energy is dissipated into the surrounding

matrix.³² Since the latter process is related to the molecular mobility of the matrix,^{13,33–35} the magnitude of k_{TS0} provides a measure of matrix mobility. Variation in lifetime thus implies variation in the dynamic environment of the Ery B probe in the different sucrose–salt films.

The analysis of the effect of temperature on lifetime indicates that the non-radiative quenching rate k_{TS0} increased gradually in the glass but dramatically in the undercooled liquid above the sucrose T_g . Addition of salt decreased the non-radiative quenching rate over the whole temperature range and the effect varied with the kind of salt. At a mole ratio of 0.2:1 (salt/sucrose), all salts except NaH_2PO_4 significantly decreased the probe's non-radiative quenching rate k_{TS0} (Figs. 2c and 3c), indicating an increase in matrix rigidity (decrease in molecular mobility) due to salt interactions with sucrose. The magnitude of the decrease in mobility was larger in the Na salts (except for NaH_2PO_4) than in the Mg and Ca salts. Effects of salt on the dynamic transition temperatures provide a further indication of the effect of salt on matrix mobility (calculated from the intersection of linear trendlines in Arrhenius plots of k_{TS0} at high and low temperature with k_{TS0} calculated from lifetimes determined during the cooling cycle). The transition temperature, discussed here, is defined as the temperature at which the large-scale cooperative molecular mobility motions are activated. The transition temperature was 76 °C in pure sucrose, significantly higher than the glass transition of sucrose (~62 °C) and 77 °C in sucrose–NaCl, 79 °C in sucrose– NaH_2PO_4 , sucrose–NaAcetate and sucrose– MgCl_2 , 80 °C in sucrose– Na_2HPO_4 , 81 °C in sucrose– $\text{Na}_3\text{Citrate}$, and 85 °C in sucrose– CaCl_2 . The increase in the transition temperatures suggests that the large amplitude α relaxations in the sucrose matrix were activated at slightly higher temperature due to strong ionic interactions between the salt ions and sucrose.

Mazzobre et al. measured the glass transition temperature of the maximally freeze-concentrated matrix (T'_g) in glassy freeze-dried trehalose and sucrose in the presence of different salts.³⁶ They found that T'_g was decreased but the actual T_g values of the systems were not modified when small amounts of salts were added (mass fraction below 0.05). Although citrate is supposed to lower the T_g of sucrose,^{37,38} Kets et al., using a modified DSC method, determined that T_g of sucrose actually increased with added citrate.³⁹ Salts were reported to increase the viscosity of sugar solutions containing polar solvents and may thus increase T_g through specific interactions such as hydrogen bonding.^{40,41} Generally, however, as indicated by the hysteresis noted above, sugar–salt mixtures retain more water than pure sugar matrixes, leading to lower glass transition temperatures for the mixture.

The differential effects of salts on matrix mobility may be the result of different interactions between these ions and sucrose. It is possible that specific sucrose–salt complexes may contribute to the reduced molecular mobility. Angyal has pointed out that in aqueous solutions metal cations are coordinated to water molecules as well as to a suitably arranged combination of 2 or 3 hydroxyl groups of carbohydrates.⁴² The complex strength depends on the types of carbohydrate and salt. He reports that the sugars common in nature do not readily form complexes and that the complexes formed between cations and neutral carbohydrates are weak.⁴² We are not aware of any reports of complexes formed between sucrose and cations in aqueous solution.

However, in the dehydrated state, the removal of water may facilitate the ability of sugar hydroxyl groups to coordinate cations. Cook and Bugg found that in hydrated solid-state environments hydroxyl groups at the O2 and O3 positions in hexose molecules served as effective Ca^{2+} -chelation sites, but this interaction was weak due to steric constraints.⁴³ Morel-Desrosiers et al. reported that Ca^{2+} has stronger interactions with sugar than Mg^{2+} , resulting in a denser or more tightly packed matrix.⁴⁴ Most of the anions in

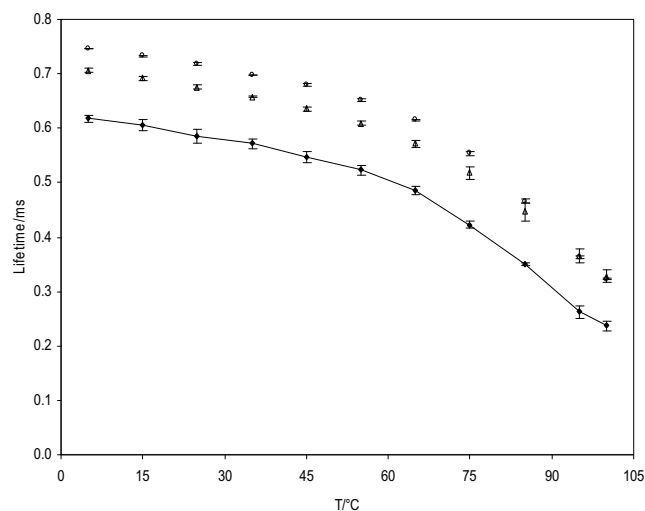


Figure 7. Phosphorescence lifetime of erythrosin B as a function of temperature in sucrose–salt films at constant Na/sucrose mole ratio: ◆, sucrose; △, sucrose– Na_2HPO_4 (0.2:1); ○, sucrose–NaAcetate (0.4:1).

the Na salts (except for Cl), however, can also form hydrogen bonds with sucrose. The probe lifetime increased in the order $\text{NaH}_2\text{PO}_4 < \text{NaAcetate}$ at a mole ratio of 0.2:1 Na/sucrose (Fig. 3a) and in the order $\text{Na}_2\text{HPO}_4 < \text{NaAcetate}$ at a mole ratio of 0.4:1 Na: sucrose (Fig. 7). These variations in mobility at constant cation concentration suggest that hydrogen bonding by the anion may play an important role in reducing matrix mobility.

3.3. Dynamic site heterogeneity

Sucrose and sucrose–salt matrixes exhibited considerable spectroscopic heterogeneity: the phosphorescence lifetime varied significantly with both excitation and emission wavelength and the extent of spectral heterogeneity varied with salt. This spectral heterogeneity is explained by proposing that Ery B molecules are distributed among sites that vary in molecular mobility and that sites with slow dipolar relaxation rates also have slow collisional quenching rates.¹³ The variation of lifetime with emission wavelength then reflects a broad continuum of local matrix sites that vary in terms of their overall molecular mobility. Probes in sites that cause a blue-shift with slower dipolar relaxation rates have longer lifetimes and thus smaller values of the collisional quenching rate k_{TS0} ; these probes are in less mobile sites. Probes in sites that cause a red-shift with faster dipolar relaxation rates, on the other hand, have shorter lifetimes and thus larger values of the quenching rate; these probes are thus in more mobile sites. An increase in spectral heterogeneity reflects an increase in dynamic site heterogeneity, and thus an increase in the extent of coupling between the rates for solvent relaxation (which modulates emission wavelength) and collisional quenching (which modulates lifetime) within the matrix.¹³

Dynamic site heterogeneity is a common characteristic of amorphous solids and supercooled liquids below and above T_g .^{45,46} Extensive research applying different physical techniques has revealed the presence of dynamically distinct regions in amorphous synthetic polymers.^{47,48} Dynamic site heterogeneity involves the presence of spatial regions within the amorphous material whose boundaries and intrinsic rates of molecular mobility fluctuate through both time and space. Recently, site heterogeneity has been detected in amorphous solids composed of sugars and sugar alcohols^{13,14,16} and both fibrous and globular proteins.^{17,20,21} Variations in molecular mobility are of interest because they may be relevant to degradation processes including physical aging^{49,50} and chemi-

cal reactions such as Asp-Pro peptide bond cleavage in Physalaeamin in freeze-dried and freeze-concentrated carbohydrates.⁵¹

Lower values of β indicate that a broader distribution of lifetimes are required to fit the phosphorescence intensity decays.⁵² Since the lifetime varies due to variations in the non-radiative decay rates, and specifically variations in the rate of collisional quenching k_{TSO} ,¹³ the magnitude of β provides a measure of variations in matrix mobility. Addition of either NaCl or any one of the other sodium salts (Figs. 2b and 3b) increased β across the entire temperature range, indicating that sodium salts tended to decrease the matrix dynamic variability; the addition of MgCl_2 and CaCl_2 , however, lowered β and thus caused an increase in matrix dynamic variability in glassy sucrose. These trends, which are also manifest in the measurements of β across the excitation and emission bands, may reflect differences in the way in which these cations interact with sugar molecules.

4. Conclusions

Salts are nearly ubiquitous in foods and biological systems, and are also widely used in solid pharmaceutical formulations. It is important to determine the effect of salts on matrix characteristics since these properties have implications for the processing and subsequent storage stability of biological materials and of foods.

The data reported here indicate that salts themselves lower the rate of collisional quenching of the erythrosin triplet state, indicating that salts lower the matrix molecular mobility (increase the local matrix rigidity). The rigidifying effect varies with the salt when monitored at a fixed salt/sucrose mole ratio of 0.2:1, with NaH_2PO_4 having essentially no measurable effect on matrix mobility and the other salts, NaCl, CaCl_2 , MgCl_2 , NaAcetate, $\text{Na}_3\text{Citrate}$, and Na_2HPO_4 , exhibiting significant effects on mobility. Due to the affinity of the salts (except NaCl) for moisture, salt-containing sucrose films exhibit significant hysteresis as the annealing effect of heating dried out the films; the magnitude of hysteresis varied with the type of salt.

Spectral heterogeneity of Ery B phosphorescence also provided direct support for a physical model of dynamic site heterogeneities within supercooled liquids and amorphous solids above and below the glass transition temperature.^{45,46} Addition of salts influenced the dynamic site heterogeneity of the amorphous sucrose matrix and this effect was dependant on the type of salt. The sodium salts in general decreased, while MgCl_2 and CaCl_2 appeared to increase the extent of dynamic heterogeneity in amorphous sucrose; additional cation salts need to be investigated to confirm the generality of this result.

5. Experimental

5.1. Sample preparation

Sucrose was purchased from Sigma–Aldrich (St. Louis, MO) with minimum purity of 99.5%. About 50 g of sucrose was dissolved in about 30 g of deionized water containing 0.77 g of activated charcoal to remove luminescent impurities. After stirring overnight, the mixture was vacuum-filtered through ashless filter paper (Whatman No. 40); 0.7 g of activated charcoal was added to the filtrate and the process was repeated. The final concentration of purified sucrose solution was adjusted to 65–67 wt % and confirmed by using a refractometer (NSG Precision Cells, Inc., Farmingdale, NY). Before preparing samples the sucrose solution was filtered through a membrane with 0.2 μm pores to remove remaining particles.

The free acid of erythrosin B (Ery B, tetra-iodo fluorescein; Sigma Chemical Co., St. Louis, MO) was dissolved in spectrophotometric grade dimethylformamide (DMF; Aldrich Chemical Co.,

Milwaukee, WI) to prepare a 10 mM stock solution; an aliquot from this solution was added to the concentrated sucrose to obtain a dye/sucrose mole ratio of 1:10⁴.

We prepared glassy sucrose films by using a slightly modified version of our previous method.¹³ In order to improve the surface activity for spreading sucrose solutions, quartz slides were washed overnight with Alconox soap, then washed with deionized water; activated for 30 min with concentrated nitric acid, then rinsed with deionized water; cleaned with 95% ethanol for 2 h and finally with deionized water again. To obtain amorphous sucrose films with Ery B, 15 μL of the sucrose solution containing Ery B at a ratio of 1:10⁴ was added on a quartz slide (30 \times 13.5 \times 0.6 mm, custom made by NSG Precision Cells, Farmingdale, NY). Another slide was placed on top of the solution and the slides were drawn horizontally past one another to form a film. The solution on the slides was then heated under a heat gun (Vidal Sassoon) for 5 min to a maximum temperature of 86–88 °C (measured using a thermocouple probe). The thickness of amorphous sucrose films prepared by this procedure ranged from 10 to 40 μm . The slides were stored against P_2O_5 and Drierite for at least 7 days and checked for crystals within the film through crossed polarizers in a dissecting microscope (Nikon Type 102, Japan) before any phosphorescence measurements.

Sucrose–salt mixtures were prepared from sucrose solution containing dye. Seven salts (sodium chloride, NaCl; calcium chloride dihydrate, $\text{CaCl}_2 \cdot 2\text{H}_2\text{O}$; magnesium chloride hexahydrate, $\text{MgCl}_2 \cdot 6\text{H}_2\text{O}$; acetic acid sodium salt trihydrate, $\text{CH}_3\text{CO}_2\text{Na} \cdot 3\text{H}_2\text{O}$; Na_3 citrate dihydrate, $\text{C}_6\text{H}_5\text{Na}_3\text{O}_7 \cdot 2\text{H}_2\text{O}$; anhydrous monobasic sodium phosphate, NaH_2PO_4 ; and sodium phosphate dibasic heptahydrate, $\text{Na}_2\text{HPO}_4 \cdot 7\text{H}_2\text{O}$; all from Sigma Chemical Co., St. Louis, MO) were added individually to the purified sucrose solutions to obtain a mixture solution with a fixed salt/anhyd sucrose mole ratio of 0.2:1. This concentration was selected to make sure that salts have observable effects on sucrose matrix without phase separation in the sucrose–salt mixtures. Prior to preparing glassy films, sucrose–salt solutions were filtered through a membrane with 0.2 μm pores. Films were then made and stored as described above.

Water content in amorphous sucrose and sucrose–salt films was determined gravimetrically (by difference of mass before and after drying for 24 h at 70 °C in an Ephorte (Haake Buchler, Inc.) vacuum oven at 1 kPa). Sample films were scratched from quartz slides and ground into powders in a glove box containing P_2O_5 and Drierite with a relative humidity less than 5%. The water contents of the films (in wt % moisture) were pure sucrose (0.56 ± 0.13), sucrose–NaCl (1.04 ± 0.01), sucrose– CaCl_2 (3.12 ± 0.42), sucrose– MgCl_2 (3.81 ± 0.98), sucrose–NaAcetate (3.50 ± 0.08), sucrose– $\text{Na}_3\text{Citrate}$ (4.08 ± 0.36), sucrose– NaH_2PO_4 (2.81 ± 0.17), and sucrose– Na_2HPO_4 (4.26 ± 0.18).

5.2. Luminescence measurements

Luminescence measurements were made using a Cary Eclipse Fluorescence spectrophotometer (Varian Instruments, Walnut Creek, CA). Prior to any phosphorescence measurements, all samples were flushed for at least 15 min with nitrogen gas which contained less than 1 ppm oxygen to eliminate oxygen quenching. The temperature was controlled using a thermo-electric temperature controller (Varian Instruments, Walnut Creek, CA). To eliminate moisture condensation during the measurements below room temperature, dry air was used to flush the chamber surrounding the cuvette holder. All the measurements were made at least in triplicate.

To obtain intensity decays of erythrosin B in sucrose and sucrose–salt mixtures, samples were excited at 530 nm (20 nm bandwidth) and emission transients collected at 680 nm (20 nm bandwidth) over the temperature range from 5 to 100 °C (heating

cycle) and then, after waiting for 10 min, from 100 to 5 °C (cooling cycle) using the same sample.

At each target temperature, samples were equilibrated for 1 min/°C increase in temperature. Phosphorescence intensity decays were collected over a window of 5 ms with an initial delay of 0.1 ms and increments of 0.04 ms. Each decay was the average of 20 cycles. Because intensity decays were non-exponential, a stretched exponential, or Kohlrausch–Williams–Watts' decay function was selected to analyze the intensity decay.^{12,13,53}

$$I(t) = I_0 \exp(-(t/\tau)^\beta) + \text{constant} \quad (1)$$

where I_0 is the initial amplitude, τ is the stretched exponential lifetime, and β is an exponent varying from 0 to 1 that characterizes the distribution of lifetimes.⁵² The use of a stretched exponential model provides a direct measure of a continuous distribution of lifetimes, which is appropriate for describing a complex glass possessing a distribution of relaxation times for the dynamic molecular processes.¹³ The smaller the β value, the more non-exponential the intensity decay and the broader the distribution of lifetimes. The program NFIT (Galveston, TX) was used to fit the decays; goodness of fit was evaluated by examining the χ^2 and R^2 values. Plots of modified residuals (defined as the difference between the intensity from the fit decay curve and the measured intensity divided by the square root of the measured intensity) was also used as an indicator of the goodness of fit. R^2 for all fits ranged from 0.99 to 1.00 and modified residuals plots fluctuated randomly around zero amplitude.

Phosphorescence emission lifetimes of Ery B as a function of emission wavelength were measured with excitation wavelength at 530 nm (20 nm bandwidth); emission wavelength varied from 640 to 720 nm (20 nm bandwidth). Phosphorescence emission lifetimes as a function of excitation wavelength were measured with emission wavelength at 680 nm (20 nm bandwidth); excitation wavelength ranged from 490 to 560 nm (20 nm bandwidth). These experiments were performed at 25 °C.

5.3. Photophysical scheme

Our analysis of the delayed emission is similar to the photophysical scheme for Ery B outlined by Duchowicz et al.³⁰ The measured emission rate for phosphorescence (k_P) is the sum of all possible deexcitation rates for the triplet state T_1 :

$$\tau^{-1} = k_P = k_{RP} + k_{TS1} + k_{TS0} + k_Q[Q] \quad (2)$$

In this equation, k_{RP} is the rate of radiative emission to the ground state S_0 . For erythrosin B, k_{RP} is 41 s^{-1} and constant with temperature.³⁰

The rate k_{TS1} is the rate of thermally activated reverse intersystem crossing from the triplet state T_1 to the singlet state S_1 ; its value can be estimated from the Arrhenius equation:

$$k_{TS1}(T) = k_{TS1}^0 \exp(-\Delta E_{TS}/RT) \quad (3)$$

where k_{TS1}^0 is the maximum rate of intersystem crossing from T_1 to S_1 at high temperature, ΔE_{TS} is the energy gap between T_1 and S_1 , $R = 8.314 \text{ J K}^{-1} \text{ mol}^{-1}$, and T is the temperature in Kelvin. The value of ΔE_{TS} is calculated from the slope of a Van't Hoff plot of the natural logarithm of the ratio of intensity of delayed fluorescence (I_{DF}) to phosphorescence (I_P):

$$d[\ln(I_{DF}/I_P)]/d(1/T) = -\Delta E_{TS}/R \quad (4)$$

where I_{DF} and I_P are the maximum intensity values determined from analysis of the emission band using log-normal line shape function as described by You and Ludescher.²⁸ The value of k_{TS1} at 25 °C, for example, is 88 s^{-1} using the parameters for pure sucrose, $k_{TS1}^0 = 3.0 \times 10^7 \text{ s}^{-1}$ and $\Delta E_{TS} = 31.56 \text{ kJ/mol}$.¹³ The values of ΔE_{TS}

varied slightly in different matrixes. For example, the value of ΔE_{TS} for NaCl/sucrose was 30.80 kJ/mol (2% smaller than ΔE_{TS} for pure sucrose). Using the value of 31.56 kJ/mol for pure sucrose, instead of the value of 30.8 kJ/mol, makes the calculated value of k_{TS1} smaller at each temperature and thus the value of k_{TS0} (the calculated mobility) higher at each temperature: ~2% higher in the glass state at low temperature and ~15% higher in the undercooled liquid state at 100 °C. In other words, our use of 31.56 kJ/mol for ΔE_{TS} means that the values of k_{TS0} , the matrix mobility, in mixtures were possibly overestimated by something in the range from 2% to 15%. Since these sucrose–salt films with a low concentration of salt (mole ratio of 0.2:1) had only slightly different values of ΔE_{TS} , the value of ΔE_{TS} for sucrose was used to calculate the value of k_{TS1} in all films.

In the presence of oxygen, the quenching rate $k_Q[Q]$ is the product of rate constant k_Q and the oxygen concentration $[O_2]$. By flushing with nitrogen throughout the measurements we ensure that no oxygen quenching occurred. One of the non-radiative decay routes is through internal conversion. This decay rate is k_{TS0} , which reflects the rate of collisional quenching of the probe due to both internal and external factors.³² We assume that the term k_{TS0} primarily reflects the external environmental factors since self collisional quenching among probe molecules can be neglected within the extremely viscous amorphous solid. The temperature-dependent term k_{TS0} can be calculated from phosphorescence lifetime by rewriting Eq. 2.

$$k_{TS0}(T) = \frac{1}{\tau(T)} - k_{RP} - k_{TS1}(T) \quad (5)$$

References

- Fennema, O. R. *Food Chemistry*, 3rd ed.; Marcel Dekker: New York, 1996; pp 17–94.
- Roos, Y. *Phase Transitions in Foods*; Academic Press: San Diego, 1995; pp 193–246.
- Slade, L.; Levine, H. *Adv. Food Nutr. Res.* **1995**, *38*, 103–269.
- Wolkers, W. F.; Oldenhof, H.; Alberda, M.; Hoekstra, F. A. *Biochim. Biophys. Acta* **1998**, *1379*, 83–96.
- Ottenhof, M.; MacNaughtan, W.; Farhat, I. A. *Carbohydr. Res.* **2003**, *338*, 2195–2202.
- Chan, R. K.; Pathmanathan, K.; Johari, G. P. *J. Phys. Chem.* **1986**, *90*, 6358–6362.
- Gangasharan; Murthy, S. S. N. *J. Phys. Chem.* **1995**, *99*, 12349–12354.
- Richert, R. *Europhys. Lett.* **2001**, *54*, 767–773.
- van den Dries, I. J.; Besseling, N. A. M.; van Dusschoten, D.; Hemminga, M. A.; van der Linden, E. J. *J. Phys. Chem. B* **2000**, *104*, 9260–9266.
- Contreras-Lopez, E.; Champion, D.; Hervet, H.; Blond, G.; Le Meste, M. *J. Agric. Food Chem.* **2000**, *48*, 1009–1015.
- Buitink, J.; van den Dries, I. J.; Hoekstra, F. A.; Alberda, M.; Hemminga, M. A. *Biophys. J.* **2000**, *79*, 1119–1128.
- Richert, R. *J. Chem. Phys.* **2000**, *113*, 8404–8429.
- Pravinata, L. C.; You, Y.; Ludescher, R. D. *Biophys. J.* **2005**, *88*, 3551–3561.
- Shirke, S.; Ludescher, R. D. *Carbohydr. Res.* **2005**, *340*, 2661–2669.
- Shirke, S.; Takhistov, P.; Ludescher, R. D. *J. Phys. Chem. B* **2005**, *109*, 16119–16126.
- Shirke, S.; You, Y.; Ludescher, R. D. *Biophys. Chem.* **2006**, *123*, 122–133.
- Lukasik, K. V.; Ludescher, R. D. *Food Hydrocolloids* **2006**, *20*, 88–95.
- Lukasik, K. V.; Ludescher, R. D. *Food Hydrocolloids* **2006**, *20*, 96–105.
- Simon-Lukasik, K. V.; Ludescher, R. D. *Food Hydrocolloids* **2004**, *18*, 621–630.
- Nack, T. J.; Ludescher, R. D. *Food Biophys.* **2006**, *1*, 151–162.
- Sundaresan, K. V.; Ludescher, R. D. *Food Hydrocolloids* **2008**, *22*, 403–413.
- Crowe, J. H.; Carpenter, J. F.; Crowe, L. M. *Annu. Rev. Physiol.* **1998**, *60*, 73–103.
- Crowe, J. H.; Oliver, A. E.; Tablin, F. *Int. Comp. Biol.* **2002**, *42*, 497–503.
- Buitink, J.; Leprince, O. *Cryobiology* **2004**, *48*, 215–228.
- Izutsu, K.; Aoyagi, N. *Intl. J. Pharm.* **2005**, *288*, 101–108.
- Shalae, E. Y.; Johnson-Elton, T. D.; Chang, L.; Pikal, M. J. *Pharm. Res.* **2002**, *19*, 195–201.
- Mazzobze, M. F.; Buera, M. P. *Biochim. Biophys. Acta* **1999**, *1473*, 337–344.
- You, Y.; Ludescher, R. D. *Carbohydr. Res.* **2008**, *343*, 350–363.
- You, Y.; Ludescher, R. D. *Appl. Spectrosc.* **2006**, *60*, 813–819.
- Duchowicz, R.; Ferrer, M. L.; Acuna, A. U. *Photochem. Photobiol.* **1998**, *68*, 494–501.
- Lettinga, M. P.; Zuillhof, H.; van Zandvoort, A. M. *J. Phys. Chem. Chem. Phys.* **2000**, *2*, 3697–3707.
- Papp, S.; Vanderkooi, J. M. *Photochem. Photobiol.* **1989**, *49*, 775–784.
- Strambini, G. B.; Gonnelli, M. *Chem. Phys. Lett.* **1985**, *115*, 196–200.
- Gonnelli, M.; Strambini, G. B. *Biochemistry* **1995**, *34*, 13847–13857.

35. Fischer, C. J.; Gafni, A.; Steele, D. G.; Schauerte, J. A. *J. Am. Chem. Soc.* **2002**, *124*, 10359–10366.
36. Mazzobre, M. F.; Longinotti, M. P.; Corti, H. R.; Buera, M. P. *Cryobiology* **2001**, *43*, 199–210.
37. Lu, Q.; Zografi, G. *J. Pharm. Sci.* **1997**, *86*, 1374–1378.
38. Wang, W. *Int. J. Pharm.* **2000**, *203*, 1–60.
39. Kets, E. P. W.; Ijpelaar, P. J.; Hoekstra, F. A.; Vromans, H. *Cryobiology* **2004**, *48*, 46–54.
40. Miller, D. P.; de Pablo, J. J.; Corti, H. R. *J. Phys. Chem.* **1999**, *103*, 10243–10249.
41. Wu, Y.; Li, L.; Liu, J.; Zhu, G. *Anal. Chim. Acta* **2005**, *539*, 271–275.
42. Angyal, S. J. *Adv. Carbohydr. Chem. Biochem.* **1989**, *47*, 1–43.
43. Cook, W. J.; Bugg, C. E. *Carbohydr. Res.* **1973**, *31*, 265–275.
44. Morel-Desrosiers, N.; Lhermet, C.; Morel, J. J. *J. Chem. Soc., Faraday Trans.* **1991**, *87*, 2173–2177.
45. Ediger, M. D. *Annu. Rev. Phys. Chem.* **2000**, *51*, 99–128.
46. Richert, R. J. *Phys. Condens. Mat.* **2002**, *14*, R738–R803.
47. Schmidt-Rohr, K.; Spiess, H. W. *Phys. Rev. Lett.* **1991**, *66*, 3020–3023.
48. Ediger, M. D.; Skinner, J. L. *Science* **2001**, *292*, 233–234.
49. Courtney, T. T.; Ediger, M. D. *J. Chem. Phys.* **2002**, *116*, 9089–9099.
50. Courtney, T. T.; Ediger, M. D. *J. Chem. Phys.* **2003**, *118*, 1996–2004.
51. Streeland, L.; Auffret, A. D.; Franks, F. *Pharm. Res.* **1998**, *15*, 843–849.
52. Lindsey, C. P.; Patterson, G. D. *J. Chem. Phys.* **1980**, *73*, 3348–3357.
53. Lee, K. C. B.; Siegel, J.; Webb, S. E. D.; Leveque-Fort, S.; Cole, M. J.; Jones, R.; Dowling, K.; Lever, M. J.; French, P. M. W. *Biophys. J.* **2001**, *81*, 1265–1274.